5th International Conference on Experimental Fluid Mechanics – ICEFM 2018 Munich
Munich, Germany, July 2-4, 2018

Turbulent convective heat-transfer measurements in boundary layers with ribs

Fermin Mallor[1,2], Marco Raiola[1], Carlos Sanmiguel Vila[1], Ramis Örlü[2], Andrea Ianiro[1], Stefano Discetti[1]*

[1] Universidad Carlos III de Madrid, Aerospace Engineering Group, Leganés, Spain

[2] Linné FLOW Centre, Dept. of Mechanics, KTH Royal Institute of Technology, Stockholm, Sweden

*sdiscett@ing.uc3m.es

Abstract

An investigation on the relation between turbulent flow features in turbulent boundary layers downstream of wall-proximity ribs and heat transfer at the wall is carried out. The objective is to detect the structures responsible for the Nusselt-number augmentation, with the final task of improving our understanding of the heat-transfer enhancement process. The measurements are carried out at a Reynolds number (based on the rib height and free-stream velocity) approximately equal to 4600, and consists of flow field and heat transfer characterization. Wall-proximity ribs with square cross-section are tested at two different gaps (0.25 and 0.5 ribs heights) and in wall-attached configuration. Heat-transfer measurements are performed implementing a time-resolved heated-thin-foil sensor, consisting of a low-thermal inertia foil located downstream of the obstacle, and Infrared (IR) thermography to capture the wall temperature at a rate of 1.5 kHz. A modal analysis based on Proper Orthogonal Decomposition is carried out to extract heat transfer modes, which are identified and ranked according to their contribution to the wall Nusselt-number variance. Modal analysis on velocity-field measurements is also carried out to discuss flow-field features in view of the obtained convective heat-transfer modes. The results show a strong relation between the energy content of convective heat-transfer and flow-field modes, as well as it highlights a correlation between heat-transfer enhancement and the presence of coherent near-wall structures.

1 Introduction

In several industrial fields, such as electronic packaging and turbomachinery, the cooling capabilities have become a technology driving factor (see, e.g. Han et al. 2012, Garimella et al. 2012) due to the need of removing high amounts of heat from compact spaces. The inclusion of obstacles and roughness elements to enhance transport in the boundary layers is common since it provides a twofold advantage, both due to the increased surface interested by the convection and to the capability of generating beneficial secondary flow structures. On the downside, the recirculation zone generated in the wake immediately downstream of wall-mounted obstacles results in a local reduction of the convective heat transfer coefficient, thus leading to the formation of hot spots (Liu et al. 2008, Giordano et al. 2012, He et al. 2016). Attempts to tackle this issue, both when dealing with 3D obstacles (e.g. cubes as in Mallor et al. 2018) and with two-dimensional ribs (Astarita and Cardone 2003, He et al. 2016), have led to some modified designs able to improve heat-transfer performances.

Recently, Mallor et al. (2018) proposed the use of perforated obstacles to change the topology of the reattaching wake past the obstacle. The proposed approach is based on creating an impinging jet past the obstacle, which locally enhances the convective heat transfer. Another suitable option to enhance the performances of spanwise ribs is represented by the use of detached wall-proximity ribs (Liou and Wang 1995), which suppress the near-wall recirculation zone downstream of the rib. However, this also causes the

tilt of the obstacle wake in the wall-normal direction (Mallor et al. 2018), resulting in a performance penalty further downstream. In their recent work He et al. (2016) report detailed flow-field and heat-transfer measurements by means of Particle Image Velocimetry (PIV) and Temperature Sensitive Paints showing that the presence of a gap between the rib and the wall promotes the formation of a wall jet, allowing to remove the hot spot immediately downstream of the rib. Proper Orthogonal Decomposition (POD) of PIV data is used to visualize the different flow structures in the wake showing that for a rib attached or very close to the wall the dominant feature is represented by a flapping motion of the wake of the rib while, increasing the gap beyond 0.5 rib heights the dominant feature is the vortex shedding from the rib which behaves like a cylinder in ground effect (Raiola et al. 2016).
The description of the flow field modes with higher turbulent kinetic energy content allows to hypothesize the sources of wall convective heat-transfer enhancement and deterioration; however, as shown by Antoranz et al. (2018), although in the present problem the internal energy can be treated as a passive scalar, the effect of the boundary conditions should be taken into account at the moment of ascertaining the sources of heat transfer enhancement from the flow field topology. The recent development of experimental approaches which allow for the time-resolved estimation of wall turbulent heat fluxes (Nakamura et al. 2013, Raiola et al. 2017) allows for the analysis of the unsteady variation of the wall Nusselt-number maps, thus complementing the description and identification of the main driving factors in the heat transfer enhancement.
This work presents a combined use of PIV and time-resolved Infrared (IR) thermography measurements, allowing to analyse both time average and instantaneous flow field and Nusselt-number variation. The complexity of the setup required for the measurement synchronization (Yamada and Nakamura 2016) is overcome by analysing the dataset with a statistical approach. A Proper Orthogonal Decomposition of the flow fields and of the wall Nusselt number maps allows to discuss the relation between the turbulent features and their thermal footprint.

2 Experimental setup

The IR thermography and PIV measurements were performed in the Göttingen type wind tunnel of the Aerospace Engineering Group at the Universidad Carlos III de Madrid (UC3M). The tunnel has a square test section of 0.4 m × 0.4 m and is capable of reaching a maximum speed of 20 m/s with a streamwise turbulence intensity below 1%. The schematic of the experimental setup is reported in Figure 1. A splitter plate with a thickness of 10 mm was mounted in the test section at a distance of 0.1 m from its back wall.
Square two-dimensional ribs with 10 mm side length L were used as obstacles. In order to characterize the boundary-layer parameters, an enhanced-resolution ensemble-PTV approach (Agüera et al. 2016, Sanmiguel et al. 2017b) is applied in a test with a clean boundary layer. The boundary-layer thickness (here defined as the position at which 99% of the freestream speed is attained) has been determined to be of 42 mm at the point where the ribs were placed ($Re_\tau = 900$) resulting in having ribs with a height equal to approximately a quarter of the local boundary-layer thickness ($L/\delta_{99} = 0.24$).
The rib was placed at three different heights H from the wall: 0, 2.5 and 5 mm, corresponding to $H/L = 0.25$ and 0.5. Measurements performed in the clean boundary layer are used as a baseline. In all the cases, the velocity of the wind tunnel was set to 7.1 m/s, obtaining a local Reynolds number equal to 4600 (using the side length as characteristic length).
A stainless steel thin foil with a thickness of 10 μm was flash mounted on the flat plate, leaving a 2 mm gap between the splitter plate substrate and the thin foil (as sketched in Figure 1b). The foil was heated with a constant heat flux by the Joule effect passing a current through it, and cooled by the air stream. Compression springs were used in order to assure the flatness of the foil. In order to obtain the convective heat-transfer coefficient, the foil was modeled as a heated thin-foil heat-transfer sensor (Carlomagno and Cardone 2010). A 10 μm foil is used to reduce the attenuation effect of the foil temperature fluctuation due to thermal inertia and conduction (Nakamura 2009). The convective heat-transfer coefficient is estimated from an energy balance through the foil (see Carlomagno and Cardone 2010 for more details). The foil was covered with a thin layer of high emissivity enamel ($\varepsilon = 0.98$) in order to reduce the uncertainty of temperature measurements performed with the IR camera. The temperature at the wall is measured using a FLIR SC4000

IR camera, using a reduced focal plane array (128 × 128 instead of 320 × 256 elements) in order to achieve a frequency of acquisition equal to 1.5 kHz, with a spatial resolution of 16 pixels/L. In order to improve the measurement of the small temperature fluctuations involved in the problem, IR images were acquired and noise fluctuations were removed with the filter developed by Raiola et al. (2017), keeping the first 200 fluctuation modes.

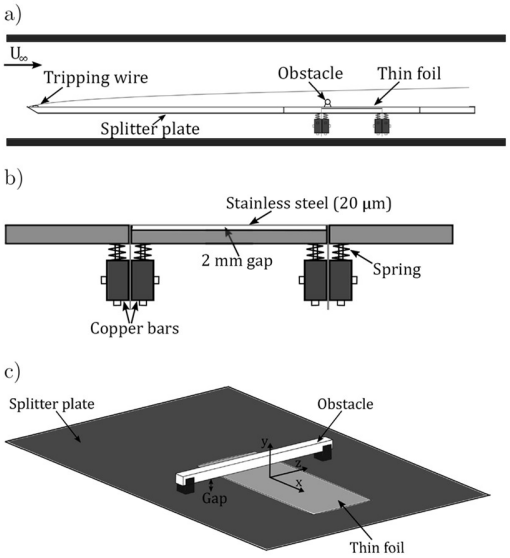

Figure 1: Sketch of the experimental set-up. a) Test section arrangement. b) Close-up of the thin foil configuration. c) Obstacle configuration and coordinate system.

The flow fields have been measured with PIV. The measurements are performed in the streamwise/wall-normal plane at the wind tunnel symmetry axis. A dual cavity Nd:Yag Quantel Evergreen laser is used in order to illuminate Di-Ethyl-Hexyl-Sebacate seeding particles. The recording device is an Andor sCMOS camera, equipped with a lens with 50 mm focal length and using a focal ratio f# equal to 11. Images were recorded with a spatial resolution of 22 pixels/mm. Sets of 2000 image pairs have been captured for each test case. The raw images were preprocessed to remove the background due to the strong reflections using an eigenbackground removal procedure (Mendez et al. 2017). A custom-made PIV software developed at the University of Naples Federico II (Astarita and Cardone 2005) was used to perform digital cross-correlation analysis of the particle images to calculate the velocity fields. The interrogation strategy is an iterative multi-grid/multi-pass image deformation algorithm, with final interrogation windows of 64 × 64 pixels with 75% overlap (the vector spacing is 16 pixels, i.e. 0.72 mm, which results in 14 vectors/L).
A POD analysis of the fluctuating flow fields and Nusselt-number distributions has been carried out in order to extract information about the turbulent coherent structures in the wake of the ribs versus those in the baseline configuration and about the main Nusselt-number modes. Spatial modes reported in the following represent an orthonormal basis and are presented in form of contour plots ranging from the minimum local values in blue to the maximum local value in red.
The uncertainty of the local Nusselt number is found to be of ±5%; the large number of snapshots used for the present investigation allows to assume a similar uncertainty for the Nusselt-number modes. For what concerns the PIV uncertainty, the PIV truncation error leads to uncertainties lower than 1%, while the large number of PIV snapshots suggests a sufficiently high convergence of flow statistics.

3 Modal decomposition of velocity field and heat transfer

The bulk of the turbulent kinetic energy is contained in the first four velocity POD modes, according to the eigenvalue distribution (not reported herein for brevity). These modes are reported in Figure 3 and are shown to be representative of large-scale sweeps/ejections. The characteristic flow features drastically change when the rib is introduced. In agreement with Mallor et al. (2018), there is a transition from a flow field dominated by Kelvin-Helmholtz (K-H) instabilities on the edges of the recirculation region for the wall-attached configuration to a regime dominated by von Kármán vortex shedding in the rib wake for the configuration of the rib detached from the wall. By the observation of the spatial modes of the flow field, reported in Figure 3 this aspect is evident; it is clear that, due to the increase of the gap between the rib and the wall, the von Kármán vortex shedding becomes more prominent and the modes acquire more coherence.

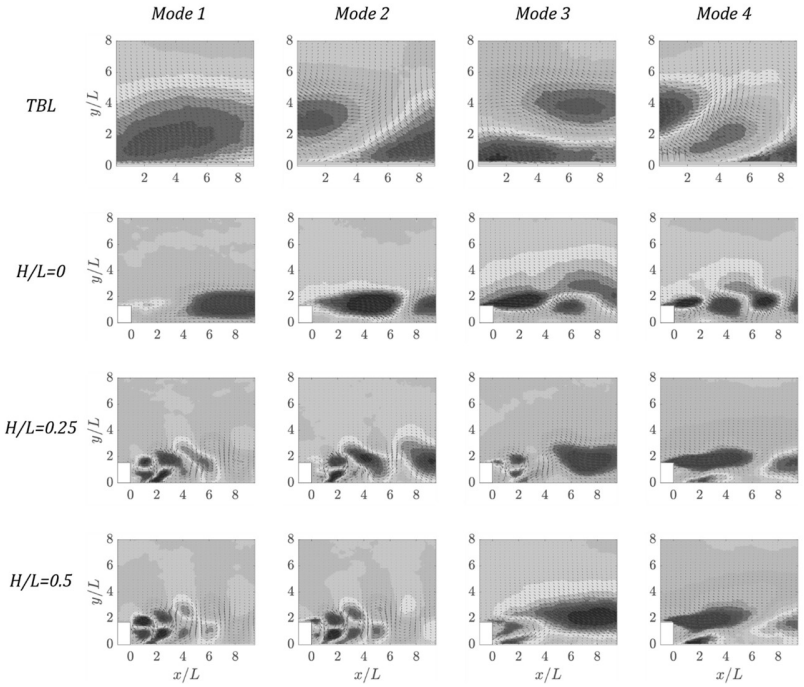

Figure 2: First four flow field modes for the four configurations under investigation: contour of normalized streamwise velocity fluctuations with superimposed vector arrows.

Regarding the heat-transfer modes, their spatial organization in the turbulent boundary layer is characterized by low/high Nusselt number streamwise streaks while, upon introducing the ribs, more coherent streamwise and spanwise oscillations are introduced. The spatial modes appear more "structured" for the case at $H/L = 0.5$ confirming that the important enhancement in the Nusselt number is due to the von Kármán shedding and, most likely, to the associated flapping of the wall jet, resulting in the first Nusselt mode, responsible of the oscillation of the location of the region of minimum Nusselt number immediately downstream of the rib. A strong relation between the coherence and strength of near-wall turbulent flow structures and the heat transfer augmentation is observed. The clean TBL is dominated by large eddies, therefore having less strength in the near-wall region, which leads to lower values of Nu. When an obstacle is introduced, the heat transfer dramatically increases. Moreover, the regions of higher augmentation can be related to the regions in which the main turbulent structures are active (shown in Figure 3): For the wall-attached case, the flow reattachment occurring at $x/L \approx 6$ leads to higher Nu augmentation downstream, whereas for the obstacles with a gap, the flapping and K-H and von Kármán vortices result in a greater augmentation closer to the obstacle (around $x/L \approx 3$).

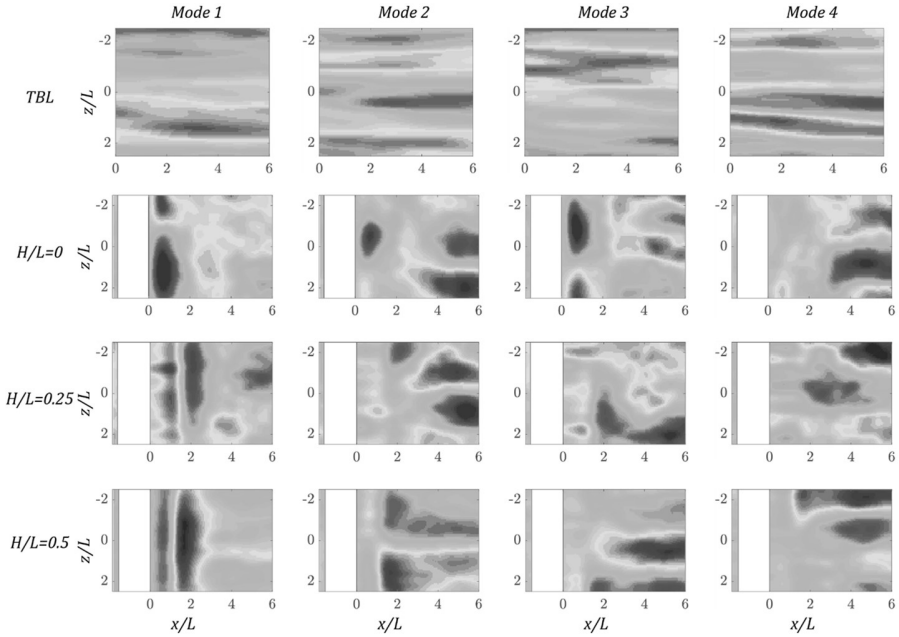

Figure 3: First four POD modes of the Nusselt number for the four tested configurations. Contour of the normalized Nu fluctuation modes.

4 Conclusion

The present study investigated the heat transfer enhancement mechanism in square wall-proximity ribs. In agreement with the literature the gap ratio $H/L = 0.5$ attains the best performance within the tested configurations. The performance enhancement is ascribed to the formation of a wall jet which is characterized by a flapping motion due to the von Kármán vortex shedding in the wake of the square ribs. This is reflected by both the increased energy content and spatial coherence of the main flow field POD modes and by the increase of the variance content and coherence of the Nusselt number spatial modes related to the wall jet flapping. The comparison of the Nusselt number spatial modes of the clean turbulent boundary layer configuration and of the configurations with the ribs shows a variation of the spatial pattern associated to oscillations with strong spanwise coherence, opposed to the thin elongated streaks which dominate the convective heat transfer in the clean turbulent boundary layer. Furthermore, a strong correlation between the convective heat transfer and the presence of highly coherent, near-wall turbulent structures is observed, leading to the conclusion that generating such structures is of high interest in the development of heat transfer systems.

Acknowledgements

This work has been partially supported by the Grant DPI2016-79401-R funded by the Spanish State Research Agency (SRA) and European Regional Development Fund (ERDF).

References

Agüera N, Cafiero G, Astarita T and Discetti S (2016) Ensemble 3D PTV for high resolution turbulent statistics. *Measurement Science and Technology* 27:124011.

Antoranz A, Ianiro A, Flores O and García-Villalba M (2018). Extended proper orthogonal decomposition of non-homogeneous thermal fields in a turbulent pipe flow. *International Journal of Heat and Mass Transfer* 118:1264-1275.

Astarita T and Cardone G (2003) Convective heat transfer in a square channel with angled ribs on two opposite walls. *Experiments in Fluids* 34:625-634

Carlomagno GM and Cardone G (2010) Infrared thermography for convective heat transfer measurements. *Experiments in fluids* 49:1187-1218.

Garimella SV, Yeh LT and Persoons T (2012) Thermal management challenges in telecommunication systems and data centers. *IEEE Transactions on Components, Packaging and Manufacturing Technology* 2:1307-1316.

Giordano R, Ianiro A, Astarita T and Carlomagno GM (2012) Flow field and heat transfer on the base surface of a finite circular cylinder in crossflow. *Applied Thermal Engineering* 49:79-88.

Han JC, Dutta S and Ekkad S (2012) Gas turbine heat transfer and cooling technology. *CRC Press*.

He C, Liu Y, Peng D and Yavuzkurt S (2016) Measurement of flow structures and heat transfer behind a wall-proximity square rib using TSP, PIV and split-fiber film. *Experiments in Fluids* 57:165.

Liou TM and Wang WB (1995) Laser holographic interferometry study of developing heat transfer in a duct with a detached rib array. *International journal of heat and mass transfer* 38:91-100.

Liu YZ, Ke F and Sung HJ (2008) Unsteady separated and reattaching turbulent flow over a two-dimensional square rib. *Journal of Fluids and Structures* 24:366-381.

Mallor F, Sanmiguel Vila C, Ianiro A and Discetti S (2018) Wall-mounted perforated cubes in a boundary layer: Local heat transfer enhancement and control. *International Journal of Heat and Mass Transfer*, 117: 498-507.

Mendez MA, Raiola M, Masullo A, Discetti S, Ianiro A, Theunissen R and Buchlin JM (2017) POD-based background removal for particle image velocimetry. *Experimental Thermal and Fluid Science* 80:181-192.

Nakamura H (2009) Frequency response and spatial resolution of a thin foil for heat transfer measurements using infrared thermography. *International Journal of Heat and Mass Transfer* 52:5040-5045.

Nakamura H and Yamada S (2013) Quantitative evaluation of spatio-temporal heat transfer to a turbulent air flow using a heated thin-foil. *International Journal of Heat and Mass Transfer*, 64:892-902.

Raiola M, Ianiro A and Discetti S (2016) Wake of tandem cylinders near a wall. *Experimental Thermal and Fluid Science* 78:354-369.

Raiola M, Greco CS, Contino M, Discetti S and Ianiro A (2017) Towards enabling time-resolved measurements of turbulent convective heat transfer maps with IR thermography and a heated thin foil. *International Journal of Heat and Mass Transfer* 108:199-209.

Sanmiguel Vila CS, Örlü R, Vinuesa R, Schlatter P, Ianiro A and Discetti S (2017) Adverse-Pressure-Gradient Effects on Turbulent Boundary Layers: Statistics and Flow-Field Organization. *Flow, Turbulence and Combustion* 99:589-612.

Yamada S and Nakamura H (2016) Construction of 2D-3C PIV and high-speed infrared thermography combined system for simultaneous measurement of flow and thermal fluctuations over a backward facing step. *International Journal of Heat and Fluid Flow* 61:174-182.